Predicting Dynamic Characteristics of the Gear Train in Laser Printers for Mechanical Halftone Banding Analysis

Wonho Lee[1], Byoungho Yoo[2] and Changbae Park[1]; [1]DMC R&D Center, Samsung Electronics Co., Ltd.; [2]Printing Solutions, Samsung Electronics Co., Ltd.; Suwon, South Korea

Abstract

The angular velocity fluctuation of the Organic Photo Conductive (OPC) drums causes the halftone banding that is a main source of the print quality degradation represented as the irregularity of the line spacing. In addition, the mechanical connections between various components in a gear train involve the fluctuation as a source of the vibration. This paper suggests modeling methods to simulate dynamic characteristics to predict the fluctuation of gears and other components affecting the banding. The model-automation tool building easily and quickly a simulation model is developed by using Finite Element Analysis (FEA) software. The usefulness of these methods is validated by the comparison with experimental results.

Introduction

The angular velocity variation of the Organic Photo Conductive (OPC) drums and the vibration of Laser Scanning Unit (LSU) in the laser exposure among the Electrophotography (EP) process cause a striped pattern called halftone banding due to scanline spacing variation. Halftone banding is an artifact of periodic light and dark bands, and affects adversely the uniformity of the printed image. In the field of our printer development, the periodic features of patterns for high frequencies sometimes distinguish jitter from banding having an irregular interval. Two types of banding are possible: the horizontal banding and vertical banding. Horizontal banding is mainly due to the vibration of LSU and the vertical banding is resulted from the fluctuations of the rotational velocity of the OPC drums, which are derived from vibration and transmission deviation induced from unstable connections among complex mechanical components, such as gear, coupler, motor, bearing, shaft, frame, and gearbox in laser printers.

Because the banding frequencies obtained from Fourier analysis of the printed images are consistent with the Gear Meshing Frequency (GMF), engineers believes that one of the main influencing factors is the Transmission Error (TE) explained by the inaccuracies geometrical errors including gear manufacturing errors such as tooth profile, lead, and runout. Moreover, it is also associated with the misalignment due to the deflection and wobble of components in a gear train [1, 2].

This paper propose a dynamic simulation modeling method for a gear train of the laser printer. We present modeling methods on many components to predict horizontal banding resulted from mechanical dynamic behaviors. Moreover, we develop a tool for model-building automation and banding frequency analysis by using commercial finite element analysis (FEA) software (Abaqus) with Python programming language [3-5]. The dynamic simulation model should include various components that play the role of providing the required torque, speed, and motion in the laser printer. Some studies have been made on the banding, but they have many restrictions in the realistic representation of multiple gears system due to limitations of analytical approach or insufficient modeling of various mechanical components [6-9]. The proposed methods and tool are focusing on predicting transient dynamic characteristics of the printer gear train and the gear angular velocity variations. Engineers can easily predict whether the image quality improves for new gear configurations.

Problem statement

Laser exposure and banding in the EP processes

Halftone banding have a relation with laser exposure in the EP process as shown in Figure 1. Researchers have shown that the vibration and the TE of a gear train resulting from mechanical components within an EP system affect the scanline spacing variation of the OPC and induce jitter or halftone banding in a printed image [6-9]. According to Chen [6], rotational velocity variations of the OPC, eccentricity and gear tooth profile error can cause the position deviation by the kinematic relation between the OPC rotation and mechanical parameters.

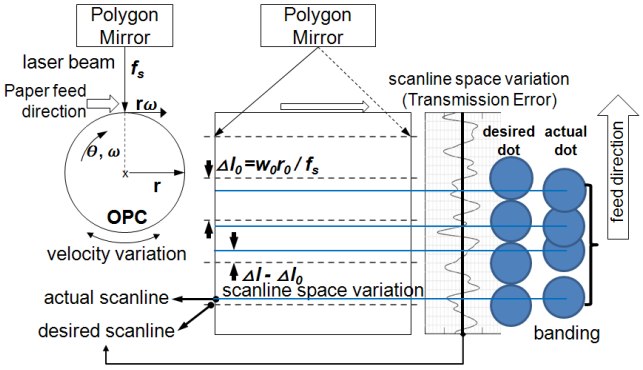

Figure 1. *Schematics for laser exposure and scanline space variation (Transmission Error) in the EP process.*

Transmission error and gear meshing frequency

The Transmission Error (TE) is an important excitation mechanism for gear noise and vibration. The definition of the TE is "The difference between the actual position of the output gear and the position it would occupy if the gear drive were perfectly conjugated [1]." This may be expressed as angular displacement or as linear displacement at the pitch point. If the gears were perfectly rigid and no geometrical errors were present, the gears would transmit the rotational motion perfectly and have no fluctuations of velocity and displacement due to no force variations. Equation (1) is the TE expressed for the angular displacement.

$$TE(t) = \theta_2(t) - \frac{N_2}{N_1}\theta_1(t) = \int \omega_2(t)dt - \frac{N_2}{N_1}\int \omega_1(t)dt \quad (1)$$

where N_1 and N_2 is the number of teeth gear 1 and gear 2. θ_1 and θ_2 is the angular displacement (radians). The ω_1 and ω_2 is the angular velocity that is a derivative of θ_1 and θ_2 with respect to time. The major causes of the TE are manufacturing errors including runout and tooth profile error as well as assembly imperfections and elastic tooth deformation, shaft, bearings, and housing. Especially, the TE is called to the Dynamic Transmission Error (DTE) in loaded and rotational status. On the effect of dynamic behaviors, the DTE is dependent on load, speed, mass, and moment of inertia. In this study, the DTE are considered, because our simulation and model is to find out the dynamic characteristics of the gear train and they include dynamic terms as stated. We mainly measure the angular velocity of gears in experiments and analyze it with FFT. In addition, the DTE is obtained from Equation (1) and its spectrum is calculated by FFT analysis.

When gears generate a meshing, the Gear Mesh Frequency (GMF) is the rate at which gear teeth mate together and equal to the number of teeth on the gear N, multiplied by the rotational cycles per second f_r (Hz) in equation (2). In the TE, the fluctuations at tooth mating appear to the GMF by the FFT analysis and the frequencies of bandings on the image is mostly consistent.

$$GMF(Hz) = N \cdot f_r \quad (2)$$

Characteristics of the printer gear train

A laser printer driving system has many mechanical components and some differences with a general industrial machine. The characteristics are described as follows:

A. Most of gears are manufactured by injection molding process and composed of rim, web, rib and bore. It has manufacturing errors such run-out according to the number of gates and the shrinkage [10].

B. An idler gear not connected to a drive shaft having a large moment of inertia has a contact between bore and stud and is rotated by slipping with stud surface. Studs do not rotate and is fixed with a frame. Clearances exist between stud and bore within 10~100 um. They can move and wobble with clearance. This motion induces axial and radial misalignment.

C. A grease is applied in clearances. Viscous resistance to grease acts on gears as a torque load.

D. A jaw type coupling connects the OPC drum with an OPC gear through surface contact mechanism. The OPC drums undergo large frictional force due to the cleaning blade so that the coupler can be deformed by torque load. Sometimes, the flexibility of coupling helps to reduce shock and vibration [1].

E. The stepped gear is used for velocity reduction. It has structure combined two gears to one body. Especially, it is useful to change helical to spur or spur to helical gear stage.

Simulation and modeling strategy

From the mechanical point of view, it is confirmed that the banding phenomenon is related to the DTE of the printer gear train. Results studied by Chen show that geometry parameters of gears affect scanline spacing variation, but they disregard the nonlinear dynamics of gear trains and considered just kinematic relations [6]. The driving system of the laser printer is so complex that predicting dynamic behaviors involved with image banding are difficult by simulation. Nevertheless, our approach introduces modeling methods that have been studied and implemented in gear and drive system fields. The strategy for banding prediction is to conduct a dynamic simulation of the printer gear train and analyze dynamic characteristics of the DTE and velocity fluctuations.

Modeling of multiple gear system

The primary components are modeled with connectors and surface elements in FEA, as shown in Figure 2. A gear train is modeled as the combination of the connector elements to impose complicated kinematic constraints for model simplification and simulation efficiency.

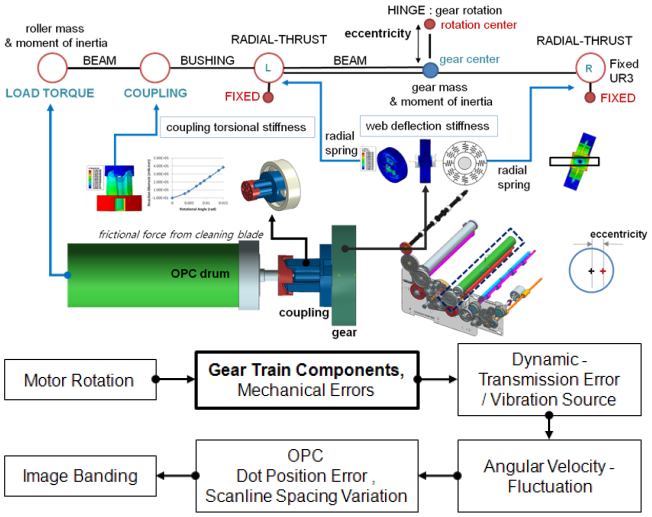

Figure 2. *Schematics of modeling components composing a gear train of a laser printer*

Deflection and contacts of gear teeth

A deflection and a deformation of gear teeth are the major factors of the TE and very important in mechanical dynamic simulation for a banding. Hence, the flexibility of the gear teeth should be described in a simulation [2, 11-14]. Figure 3 (a) is the schematic of tooth deformation. The total deformation is the sum of surface contact deformation and tooth deflection at a load condition. We can obtain a relation from FEA or Terauchi's equation that is a simplified formula to compute the tooth deformation considering the Hertzian contact deformation and the tooth deflection based on elastic deformation theory behalf of structural analysis [15, 16]. Our approach is that gears are presented with rigid shell elements for computational efficiency on behalf of solid element. Generally, rigid-body contacts do not allow penetrating surfaces to each other. However, the core of this idea is allowing penetrations to represent the tooth flexibility as the tooth deformation calculated from any tooth deformation analysis. The penalty method among contact algorithms of FEA can adjust a relationship between contact pressure and penetration, the contact stiffness [5].

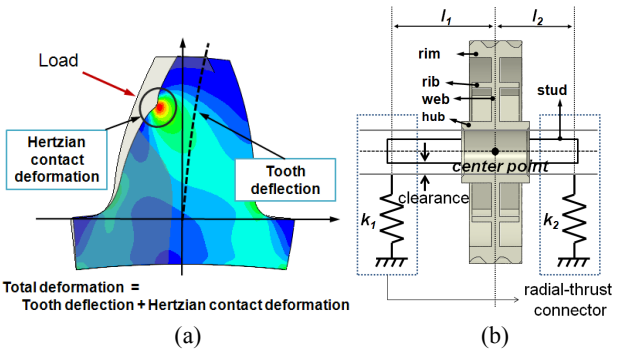

Figure 3. Schematics of the gear tooth and web deformation modeling.

Modeling of a coupling, motor pinion, gear manufacturing errors, etc.

A coupling transmits power through surface contacts and is deformed elastically. Torsional deformation is modeled using bush connectors with rotational elastic property. The torsional stiffness, which is a relation with moment and angular displacement, is obtained from FEA as shown in Figure 2.

A motor is attached to the frame, and its pinion receives the biggest moment load from connected gears in the gear train. Thus, the deformation of a frame or pinion can be caused. For the convenience of modeling, we assume that all the deformations occur in the root of a motor pinion. The bending stiffness is calculated by FEA.

Molded injection gears including rim, web and rib structure are profitable in the injection process. The axial direction load of helical gears may easily deflect thin web and rib. The deflection results in misalignment of gear and affects badly TE due to unbalanced load distributes on the tooth's surface [2]. We implement web deflection by using the radial-thrust connectors at both ends of gear bore as shown in Figure 3 (b). The radial-thrust connector has a nonlinear spring in the radial direction. The spring stiffness can be computed from FEA. When a load acts on the tooth surface, gear will deflect on the z-axis. If angular displacement and axial load were known, spring k_1 and k_2 can be calculated.

Runout and tooth profile error of injection molded gears are implemented by moving from the position of points consisting of ideal involute profiles to the position to which errors measured by experiments applied, when the in-house model-building automation tool creates geometries and an assembly [3-5, 17].

The Fourier analysis of the fluctuation of the rotational velocity and image banding

The Fast Fourier Transform (FFT) algorithm is used to analyze the fluctuation frequencies for a difference between desired angular velocity and actual angular velocity. As a result, the GMF as the source of banding and the magnitudes are computed by FFT. In addition, factors and gears related to banding can be inferred from the magnitude of the fluctuation frequencies of each component. The harmonic frequencies of the GMF in the results occur due to contact noises and numerical errors. Providing that the frequencies are unconcerned, we can use low-pass filters such as Butterworth and Chebyshev.

Experiment and application

In this chapter, the proposed model is applied to the factor analysis of the banding improvement of an entry-level mono laser printer. We reveal the improvement factor by utilizing the proposed methods, compare the simulation and experiment, and show the application and usefulness of the proposed methods.

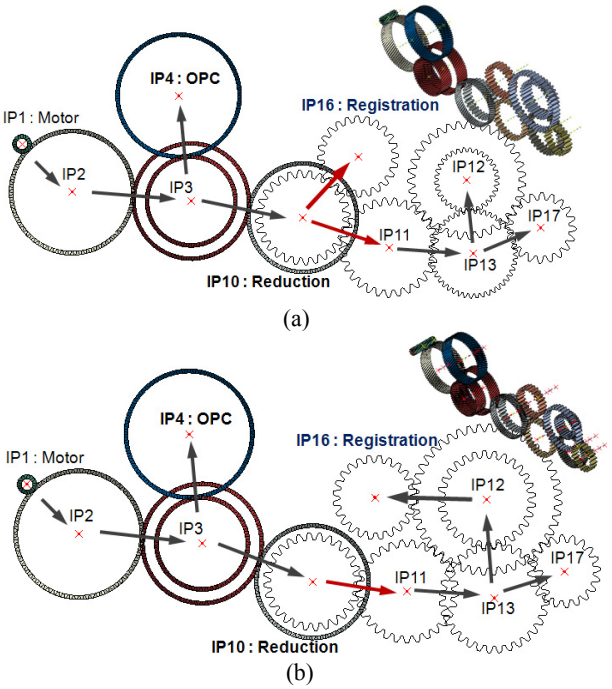

Figure 4. The gear train configurations of the original (a) and improved (b) design.

Problem statement for the application

The banding of the laser printer has been improved by modifying its gear train configurations. In the original design, the result of image banding analysis is the top shown in Figure 8. The dominant banding frequency of 116Hz was confirmed. According to the Contrast Sensitivity Function (CSF), the magnitude of a banding frequency above about 200Hz does not almost affect the human eyes at the process speed (214.13mm/s) [18, 19]. Diverse revisions to solve this problem were proposed by trial-and-error and the improved design was finalized. The image analysis result of the improved design is the top shown in Figure 9. The magnitude of 116Hz is reduced rather than the original design (0.14 to 0.097). However, engineers who are responsible for improvement still did not know the exact factors of improvement. We conducted the simulation and modeling of the laser printer and concluded that the main factor is the misalignment of IP10 gear. The detailed reasons are described below.

The differences between the original and improved design are the position and specifications of gears. Figure 4 illustrates gear train configurations of the original design (a) and the improved design (b). The banding frequency of 116Hz is identical to the GMF of IP11, IP12, IP16, and IP17. The GMF and its harmonics of other gears are detected in the image analysis results, respectively. In other words, gears having the GMF of 116Hz are

related to the banding of 116Hz, and their TE and the angular velocity variation should be reduced for repressing the banding. The engineer's intention of the improved design may be reducing transmission path from IP10 to IP16 by moving the position and connecting directly IP16 to IP10, because IP16 has a torque and can directly affect the TE. However, how it works, why the banding is reduced, and what is its mechanism is not clear.

Generating an initial simulation model and comparison with experiments

The proposed tool generates automatically the initial simulation model of the original design shown in Figure 4 (a). It requires the information of the gear train that is specifications, positions, connected components (OPC, pinion, etc.) of the gears. We use the Laser Doppler Velocimetry (LDV) to measure the velocity of gears. The angular velocity of gears is calculated by dividing the measured surface velocity with the distance from a gear center to a point measured on the gear surface.

The gear angular velocities of simulation on the original design were correlated with the velocities obtained from experiments. The FFT analysis was conducted to obtain the magnitude spectrum of the GMF on the gear angular velocity. Although the pinion and web stiffness is calculated by FEM of structural analysis, they need to be adjusted slightly to coincide the frequency-magnitude tendency with the result of experiments through parameter study. Figure 7 (a) and (b) shows that the FFT results of the gear angular velocity for the original design in simulation and experiment. Due to modeling abbreviations and measurement errors, the magnitudes of the frequencies do not exactly agree with experiments. However, the simulation results have good coherence for the increasing and decreasing relation of magnitude transmitting one gear to another, and we have confidence in the validity of the simulation and model.

Frequency isolation characteristic

One of the interesting facts discovered during the simulation of the original design is that the magnitude of 116Hz is dramatically decreased at IP10 (IP11: 0.48 to IP10: 0.1rad/s). This phenomenon is confirmed in Figure 5. Generally, engineers have the interest only for the OPC drum angular velocity variations so that has just measured it. In fact, they were not able to verify how the interested frequency component varies and what affected it due to only the measurement of the OPC angular velocity. The simulation provides the fluctuations of all gears in a gear train. From the results of the original design simulation, we observed that the magnitude of 116Hz has an abrupt change at IP10. To verify this phenomenon, the additional experiments were conducted for other gears as well as IP10 that can measure the surface velocity. From the measurements, the characteristic similar to the simulation result is verified (IP11: 0.2 to IP10: 0.07rad/s). Figure 5 shows the magnitude spectrums that are the FFT analysis results of the simulation and experiment for IP3, IP10, and IP11 of the original design. Aspects of the magnitude variation for the GMFs of the simulation seem very similar to one of the experiments. We observed the perfectly same phenomenon in the improved design, too. Consequently, we focused on the mechanical structure associated to IP10 as an isolator of the GMF components of spur gears.

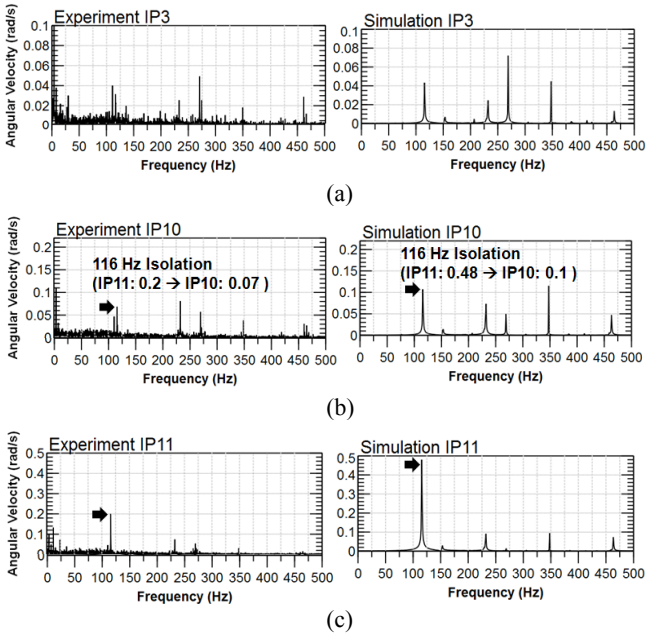

Figure 5. *The isolation characteristic of IP10 gear in the original design.*

Supporter deflection and misalignment

The stud connected with IP10 and IP11 is the cantilever structure unlike others supported on both ends of the stud (see Figure 6 (a)). Loads that a gear receives induce the stud deflection anchored at only one end. The deflection can be a cause of misalignment so that the TE amplitude may increase. This characteristic is represented by unbalanced stiffness of web deflection, which lower stiffness than k1 stiffness is used to k2 in Figure 3(b). The stiffness values are calculated by FEA.

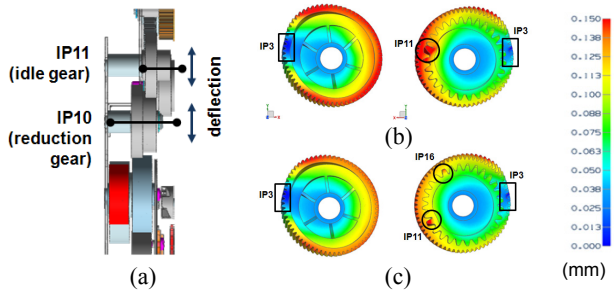

Figure 6. *The deflection of IP10 gear using FEA.*

IP10 is connected with IP3 and IP11 in the original design, but it is connected with IP3, IP11, and IP16 in the improved design. If the total torque at IP10 is equal, the deflection and wobble can depend on the location and distribution of tooth loads. Figure 6(b) and (c) show the IP10 gear deflection on the original and modified design analyzed with static structural analysis using FEM. The tooth loads divided into two in the improved design are more profitable so that the deflection in the improved design is less than in the original design. In particular, IP10 is a stepped gear combined with helical and spur gear. Generally, a spur gear does

not have an axial load resulting in misalignment. In contrast, a helical gear has it due to helical angle (20°) of the tooth surface. By the way, the spur gear of the stepped gear receives directly the axial load because of the body combined with the helical gear. Therefore, the misalignment of IP10 can affect the TE of the spur gear series (IP11, 12, 16, and 17) as very sensitive components. The effectiveness of clearance is the same.

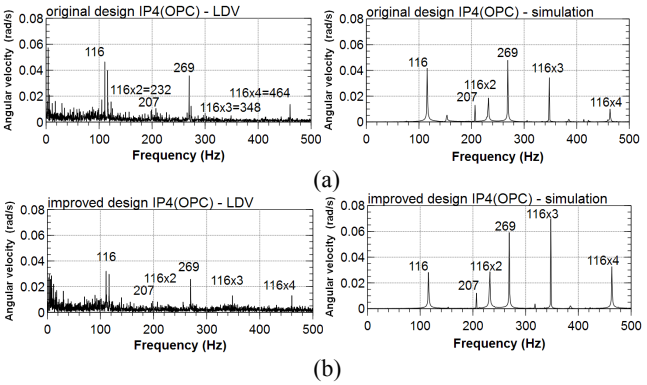

Figure 7. *The comparison of the original and improved design for the OPC gear angular velocity variation.*

Dynamic simulation of the improved design

To verify that the main factor is misalignment resulted from the difference of the load distribution in the IP10 supporting structure, we conducted simulation for the improved design.

The effect of the web deflection of IP10 and the cantilever stud of IP10 and IP11 is implemented using the nonlinear radial spring for representing web deflection and wobble. The radial spring stiffness values in Figure 2 and 3 (b) are obtained from FE structural analysis. Figure 7 (b) is the FFT analysis results of the angular velocity variation for the OPC gear obtained from the experiment and simulation, respectively. The magnitude of 116Hz in the improved design is smaller than in the original design like the LDV experiments (compare Figure 7 (a) and (b)).

FFT analysis for transmission error: comparison with the image band analysis

The previously mentioned image analysis uses the Visual Banding algorithm of the Image Quality Analyzer (IQA) system developed by our Printing solutions division [18, 19]. The fluctuation of the DTE should be analyzed in direct comparison with the image analysis of a printed image, because the DTE is a value integrated the angular velocity with respect to time, and it means the scanline spacing variation of the OPC drums. The image analysis results provide reflective lightness with respect to rotation frequency and are comparable with the scanline spacing variation. In Figure 8 and 9, the image analysis results seem very similar to the DTE spectrums, respectively. Moreover, the DTEs with respect to time have the same meanings with the scanline spacing variation in Figure 1. It presents that the proposed modeling methods and simulation can explain the OPC scanline spacing variation sufficiently.

We concluded that the improvement factors of the new design are as follows:

- ✓ The dominant banding frequency of 116Hz is induced from the GMF of the spur gear (IP11, IP12, IP16, and IP17).
- ✓ In IP10 gear, the large reduction of the magnitude of 116Hz was observed from simulations and LDV experiments. IP10 gear plays a role as an isolator of the GMF 116Hz.
- ✓ The difference between the original and improved design is the load distribution of IP10. The supporting structure of IP10 and IP11 is the cantilever type and its misalignment is induced by the flexibility and the load distributions.
- ✓ We verified that these factors affect the magnitude of 116Hz from simulation results. In addition, the tendency of simulation results agrees with experiments.

Figure 10 denotes that the magnitude of 116Hz is significantly decreased when the web stiffness is higher than current values. Therefore, the simulation verifies that if the designer reduces the deflection and misalignment of IP10 and IP11, the banding of 116Hz decreases.

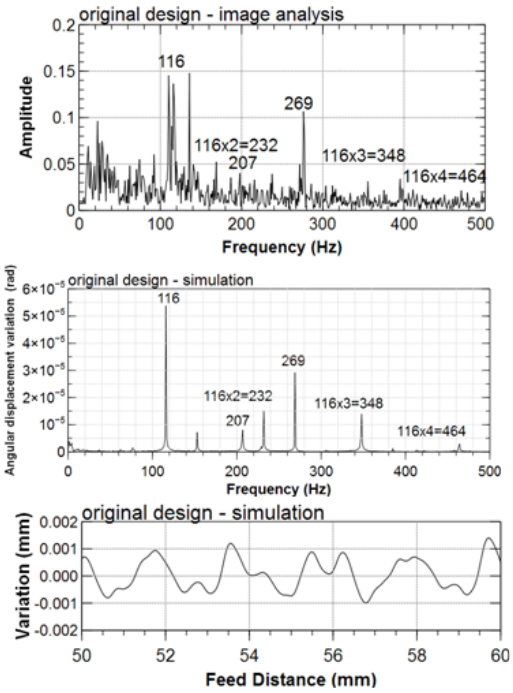

Figure 8. *The DTE (angular displacement variation) and the FFT analysis comparison of image and dynamic simulation of the OPC gear: the original design.*

CONCLUSION

Halftone banding artifacts are resulted from the OPC drums angular velocity fluctuation induced by imperfect mechanical dynamic transmission. We proposed the modeling and simulation methods to predict dynamic characteristics related to halftone banding of a printed image. The printer gear train components are modeled to represent appropriate dynamic behaviors by finite element method using commercial software. Moreover, a customized in-house model-building automation tool for engineers to generate a simulation model was developed.

Using the proposed methods, we discovered the banding improvement factor of the improved design for an entry-level mono laser printer. The GMF of the banding frequency was observed in both the simulation and experiment. Especially, by simulation, we inferred the key factor related to the difference of the DTE between the original and improved design. Finally, we revealed that the structural advantage of the improved design is low deflection of the idler stepped gear that induces a misalignment increase. With this application, the proposed method was validated by the results of many experiments and simulations. Thus, this tool provides important values in terms of the simulation to the gear train designers for evaluating designs. Our final goal is integrating developed simulation methodologies for printers including path, wrinkle, curl, motor control, and gear train.

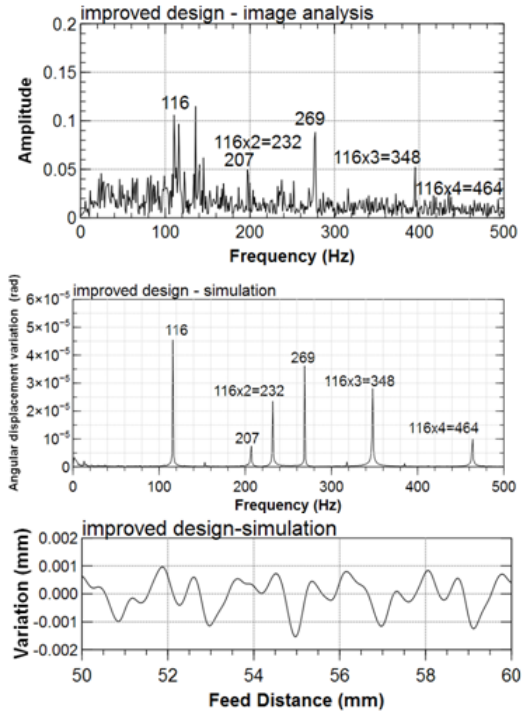

Figure 9. *The DTE (angular displacement variation) and the FFT analysis comparison of image and dynamic simulation on the OPC gear: the improved design.*

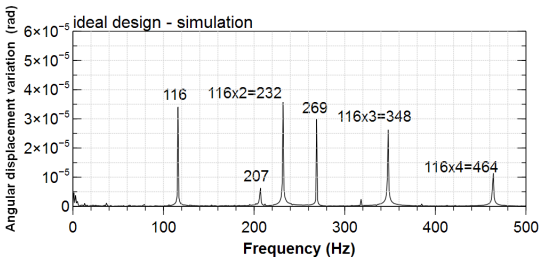

Figure 10. *The FFT analysis of the DTE on the OPC gear: the ideal design.*

References

[1] Smith, J. D. Gear noise and vibration (Marcel Dekker, 2003)

[2] M.S. Abbes, "Dynamic behaviour modelling of a flexible gear system by the elastic foundation theory in presence of defects," European Journal of Mechanics A/Solids, 29 ,5, pg. 887. (2010)

[3] Python Programming Language, http://www.python.org

[4] NumPy, SciPy, http://numpy.scipy.org

[5] Abaqus v6.10 Theory Manual (Dassault Systems, 2010)

[6] C.L. Chen, G.T.-C. Chiu, J.P. Allebach, "Halftone banding reduction for a class of electrophotographic systems - part I: characterization and modeling, " Journal of Mechatronics, doi:10.1016/j.mechatronics.2008.03.004

[7] T. Hashimoto, T. Andoh, "A Study on mechanism of local dot positioning errors cause by a paper fed into second transfer, " NIP25, pg. 707. (2009)

[8] M. Deguchi , M. Inoke, H. Inoue, M. Motegi, "Jitter analysis of printer gear, " IIP2000, JSME, pg. 37. (2000)

[9] W. Zhang, K. Karano , T. Koyama, "A Study on jitter of serial printer : vibration control of carriage system by dynamic vibration absorbers, " Trans. JSME C70, 693, pg. 1244. (2004)

[10] A. Luscher, D. Houser, "An investigation the geometry and transmission error of injection molded gears, " Journal of Injection Molding Technology 4, pg. 177. (2000)

[11] Y. Hu, Y. Shao, Z. Chen, M. Zui, "Transient meshing performance of gears with different modification coefficients and helical angles using explicit dynamic FEA, " Mechanical Systems and Signal Processing 25, pg. 1786. (2011)

[12] A. Palermo , D. Mundo, A.S. Lentini, "Gear noise evaluation through multibody TE-based simulations," Proc. ISMA2010, pg. 3033. (2010)

[13] V.K. Amabarisha, R.G. Parker, "Nonlinear dynamics of planetary gears using analytical and finite element models," Journal of Vibration and Acoustics," doi:10.1016/j.jsv.2006.11.028

[14] K. Umezawa, T. Sato , J. Ishikawa, "Simulation on rotational vibration of spur gears," Bulletin of JSME 27(223), pg. 102. (1984)

[15] Y. Terauchi, N. Kazuteru, "Study on deflection of spur gear teeth (1st report) ," Bulletin of JSME 23(184), pg. 1682. (1980)

[16] Y. Terauchi, N. Kazuteru, "Study on deflection of spur gear teeth (2nd Report)," Bulletin of JSME 24(188), pg. 447. (1981)

[17] S.Y. Kim, M.B. Shim, "Correction of the Color Registration Error Through Adjustment of Installation Phases of Gears with Runout," NIP24, pg. 726. (2008)

[18] T.H . Ha, J.P. Allebach, D.S. Cha, "Mesasument and analysis of banding artifacts in color electrophotographic printers," NIP24, pg. 463. (2008)

[19] K.Y. Lee, Y.B. Bang, H.K. Choh, New measurement method of banding using spatial features for laser printers, Proc. SPIE 7529, 75290H. (2010)

Author Biography

Wonho Lee received his BS degree from Pukyung National University (2005), and his MS degree from Ajou University (2010), all in mechanical engineering. He has been working on developments of new simulation methods for various products at Samsung Electronics DMC R&D Center. His work focused on MCAE of the laser printer.

Byoungho Yoo received his BS & MS in Naval Ocean Engineering from the Seoul National University (1996). Since then he has worked in the Noise & Vibration Research Lab. at Hyundai Heavy Industries in Ulsan, South Korea and has worked onMCAE including paper-path dynamics at Samsung Electronics Printing solutions division.

Changbae Park received his BS & MS in Mechanical Engineering from Inha University (1994). He joined Samsung Electronics in 2000 and has worked on mechanical CAE at DMC R&D Center . His work focused on noise and vibration engineering.